Jefferson.

Thomas Jefferson University
Jefferson Digital Commons

Department of Cancer Biology Faculty Papers | Department of Cancer Biology

5-11-2012

Signal transducer and activator of transcription-5 mediates neuronal apoptosis induced by inhibition of Rac GTPase activity.

Trisha R Stankiewicz
University of Denver

F Alexandra Loucks
Veterans Affairs Medical Center, Denver,

Emily K Schroeder
Veterans Affairs Medical Center, Denver,

Marja T Nevalainen
Kimmel Cancer Center, Thomas Jefferson University, marja.nevalainen@jefferson.edu

Kenneth L Tyler
University of Colorado Denver

See next page for additional authors

Let us know how access to this document benefits you

Follow this and additional works at: http://jdc.jefferson.edu/cbfp

Part of the Amino Acids, Peptides, and Proteins Commons

Recommended Citation
Stankiewicz, Trisha R; Loucks, F Alexandra; Schroeder, Emily K; Nevalainen, Marja T; Tyler, Kenneth L; Aktories, Klaus; Bouchard, Ron J; and Linseman, Daniel A, "Signal transducer and activator of transcription-5 mediates neuronal apoptosis induced by inhibition of Rac GTPase activity." (2012). *Department of Cancer Biology Faculty Papers.* Paper 28.
http://jdc.jefferson.edu/cbfp/28

This Article is brought to you for free and open access by the Jefferson Digital Commons. The Jefferson Digital Commons is a service of Thomas Jefferson University's Center for Teaching and Learning (CTL). The Commons is a showcase for Jefferson books and journals, peer-reviewed scholarly publications, unique historical collections from the University archives, and teaching tools. The Jefferson Digital Commons allows researchers and interested readers anywhere in the world to learn about and keep up to date with Jefferson scholarship. This article has been accepted for inclusion in Department of Cancer Biology Faculty Papers by an authorized administrator of the Jefferson Digital Commons. For more information, please contact: JeffersonDigitalCommons@jefferson.edu.

Authors
Trisha R Stankiewicz, F Alexandra Loucks, Emily K Schroeder, Marja T Nevalainen, Kenneth L Tyler, Klaus Aktories, Ron J Bouchard, and Daniel A Linseman

This article is available at Jefferson Digital Commons: http://jdc.jefferson.edu/cbfp/28

As submitted to:

Journal of Biological Chemistry

And later published as:

Signal Transducer and Activator of Transcription-5 Mediates Neuronal Apoptosis Induced by the Inhibition of Rac GTPase Activity*

Volume 287, Issue 20, May 2012, pp. 16835-16848

DOI: 10.1074/jbc.M111.302166

Trisha R. Stankiewicz[1,†], F. Alexandra Loucks[2,†], Emily K. Schroeder[2], Marja T. Nevalainen[3], Kenneth L. Tyler[4], Klaus Aktories[5], Ron J. Bouchard[2], Daniel A. Linseman[1,2,6]

[1]Department of Biological Sciences and Eleanor Roosevelt Institute, University of Denver, Denver, CO 80208

[2]Research Service, Veterans Affairs Medical Center, Denver, CO 80220

[3]Department of Cancer Biology and Kimmel Cancer Center, Thomas Jefferson University, Philadelphia, PA 19107

[4]Department of Neurology, University of Colorado Denver, Aurora, CO 80045

[5]Institute of Experimental and Clinical Pharmacology and Toxicology, Albert-Ludwigs-Universität Freiburg, D79104 Freiburg, Germany

[6]Division of Clinical Pharmacology and Toxicology, Department of Medicine and Neuroscience Program, University of Colorado Denver, Aurora, CO 80045

[†]These authors contributed equally to the manuscript

*Running title: *Rac inhibition induces STAT5-dependent neuronal apoptosis*

To whom correspondence should be addressed. Daniel Linseman, PhD, Veterans Affairs Medical Center, Research-151, 1055 Clermont Street, Denver CO, 80220, USA. E-mail: Dan.Linseman@va.gov.

Keywords: Janus kinase; Signal transducer and activator of transcription; Rac GTPase; Bcl-xL; apoptosis

Background: Rac GTPase functions to promote survival in primary cerebellar granule neurons.
Results: Rac GTPase inhibition induces STAT5 activation, recruitment of STAT5 to the Bcl-xL promoter, and STAT5-dependent apoptosis.
Conclusion: A novel pro-apoptotic JAK/STAT5 pathway is activated downstream of Rac GTPase inhibition in neurons.
Significance: This is the first study to implicate STAT5 as a pro-apoptotic factor in neurons.

SUMMARY

In several neuronal cell types, the small GTPase Rac is essential for survival. We have previously shown that the Rho family GTPase inhibitor, *Clostridium difficile* toxin B (ToxB)[1], induces apoptosis in primary rat cerebellar granule neurons (CGNs) princi-pally via inhibition of Rac GTPase function. In the present study, incubation with ToxB activated a pro-apoptotic Janus kinase (JAK)/signal transducer and activator of transcription (STAT) pathway and a pan-JAK inhibitor protected CGNs from Rac inhibition. STAT1 expression was induced by ToxB; however, CGNs from STAT1 knock-out mice succumbed to ToxB-induced apoptosis as readily as wild-type CGNs. STAT3 displayed enhanced tyrosine phosphorylation following treatment with ToxB and a reputed inhibitor of STAT3, cucurbitacin (JSI-124), reduced CGN apoptosis. Unexpectedly, JSI-124 failed to block STAT3 phosphorylation and CGNs were not protected from ToxB by other known STAT3 inhibitors. In contrast, STAT5A tyrosine phosphorylation induced by ToxB was suppressed by JSI-124. In addition, roscovitine similarly inhibited STAT5A phosphorylation and protected CGNs from ToxB-induced apoptosis. Consistent with these results, adenoviral infection with a dominant negative STAT5 mutant, but not wild type STAT5, significantly decreased ToxB-induced apoptosis of CGNs. Finally, chromatin immunoprecipitation with a STAT5 antibody revealed increased STAT5 binding to the promoter region of pro-survival Bcl-xL. STAT5 was recruited to the Bcl-xL promoter region in a ToxB-dependent manner and this DNA binding preceded Bcl-xL downregulation, suggesting transcription-al repression. These data indicate that a novel JAK/STAT5 pro-apoptotic pathway significantly contributes to neuronal apoptosis induced by the inhibition of Rac GTPase.

Rho family GTPases are important mediators of cellular development, survival, and death. The most well characterized members of the family are RhoA, Rac1, and Cdc42. Although best known for regulating actin cytoskeletal dynamics, Rho GTPases also play important roles in cell cycle progression (1), gene transcription (2), and cell-cell or cell-matrix adhesion (3,4). In recent years, the role of Rho GTPases in neuronal survival has begun to be investigated. For example, inhibitors of 3-HMG-CoA reductase (statins) decrease the localization of Rho GTPases to the plasma membrane and induce apoptosis in rat cortical neurons (5). We have previously shown that the function of Rac is essential for the survival of CGNs as inhibition of Rac with either large Clostridial cytotoxins or overexpression of a dominant-negative Rac mutant induces mitochondrial-dependent apoptosis of these cells (6). In a similar manner, either dominant negative Rac or siRNA against the Rac guanine-nucleotide exchange factor (GEF) alsin (ALS2) results in apoptosis of primary cultured spinal motor neurons (7). The critical role of Rac in neuronal survival is further evidenced by the finding that ALS2 is mutated in juvenile onset ALS. Although changes in Rac activity in patients harboring disease-causing ALS2 mutations have not been directly evaluated, disruption of Rac function as a possible underlying cause of neurodegenerative disease is suggested by the fact that alsin mediates Rac-dependent pro-survival signaling in primary motor neurons (7). Collectively, these findings implicate Rac as a crucial mediator of neuronal survival and suggest that disruption of Rac activity may contribute to the progression of neuro-degenerative disorders.

We have previously reported that inhibition of Rho GTPases with ToxB, and in particular inhibition of Rac, leads to the derepression of an as yet undefined, pro-apoptotic JAK/STAT pathway (8). The JAK/STAT pathway has been shown to play a critical role in cytokine signaling and JAK activation can turn on an array of downstream effects including cell proliferation, differentiation, and apoptosis (9). An important feature of the JAK/STAT signaling cascade is that it can exert either a pro-survival or pro-apoptotic effect depending upon the stimulus and cell type. For example, cytoprotective signals are transmitted from the gp130 receptor to a pro-survival JAK/STAT3 pathway in cardiac myocytes (10). Moreover, data implicate constitutive activation of STAT1 and STAT3 proteins in breast cancer cells (11). Conversely, more recent data have emerged to suggest that the JAK/STAT pathway may also induce apoptosis under certain cellular conditions. For instance, STAT1 has been shown to mediate IFN-γ induced apoptosis in liver cells treated with the heptatotoxic compound galactosamine (12). In addition, chromatin immunoprecipitation experiments performed in thymocytes suggest that glucocorticoids induce apoptosis through repression of pro-survival Bcl-xL in a STAT5-dependent manner (13). While it is clear

that JAK/STAT activation can induce apoptosis in diverse non-neuronal cell types, the significant involvement of this signaling pathway in neuronal apoptosis has only recently been recognized.

In a previous study, we showed that inhibition of Rac induces CGN apoptosis by inactivating a pro-survival p21-activated kinase (PAK)/MAP kinase kinase (MEK)/extracellular signal-regulated kinase (ERK) cascade. Although we have demonstrated that disruption of this pathway results in the derepression of a pro-apoptotic JAK/STAT pathway, we have yet to identify which particular STAT family members mediate neuronal apoptosis in response to ToxB (8). Thus, the current study focuses on identifying the STAT family members involved and the consequences of STAT activation downstream of Rac inhibition in CGNs. These primary neuronal cultures are extremely homogeneous and have been used extensively to examine molecular mechanisms involved in neuronal apoptosis (6,14-16). While we show that Rac inhibition leads to the upregulation of STAT1 expression and enhanced tyrosine phosphorylation of STAT3, we report that these transcription factors are not responsible for inducing apoptosis in ToxB-treated CGNs. Instead, we demonstrate that STAT5 is activated and subsequently translocates into the nucleus to transcriptionally repress pro-survival Bcl-xL in Rac-inhibited CGNs. To our knowledge, these results are the first to identify a pro-apoptotic function for STAT5 in primary neurons.

EXPERIMENTAL PROCEDURES

Reagents - *Clostridium difficile* toxin B was isolated or prepared as a recombinant protein as previously described (17). The polyclonal antibodies used for immunoblotting STAT1, STAT3, and phosphorylated STAT5 (pSTAT5) were from Cell Signaling (Beverly, MA, USA). Horseradish peroxidase-linked secondary antibodies and reagents for enhanced chemi-luminescence detection were from Amersham (Piscataway, NJ, USA). The polyclonal antibody used to detect active caspase-3 by immunocytochemistry was from Promega (Madison, WI, USA). For western blotting, active caspase-3 was detected with a polyclonal antibody from Abcam (Cambridge, MA, USA). 4,6-Diamidino-2-phenylindole (DAPI), Hoechst dye 33258, and a monoclonal antibody against β-tubulin were from Sigma (St Louis, MO, USA). Anti-rat and anti-mouse Cy3- or FITC-conjugated secondary antibodies for immunofluorescence were from Jackson Immunoresearch Laboratories (West Grove, PA, USA). The monoclonal antibody against Lap-2 and the polyclonal total STAT1 and total STAT5 antibodies used for western blotting were from BD Biosciences (San Diego, CA, USA). Purvalanol A, JSI-124, roscovitine, mifepristone, JAK3 inhibitor, and the small molecule JAK inhibitor I [2-(1,1-dimethyl)9-fluro-3,6-dihydro-7H-benz[h]-imidaz{4,5,-f]iso-quinolin-7one; pan-JI] were from Calbiochem (San Diego, CA, USA). The specific JAK1/2 inhibitor Ruxolitinib was purchased from ChemieTek (Indianapolis, IN, USA) and the JAK3 inhibitor Tofacitinb was from Selleck Chemicals (Houston, TX, USA).

CGN culture - Rat cerebellar granule neurons (CGNs) were isolated and cultured from 7-day-old Sprague-Dawley rat pups of both sexes (15-19 g) as previously described (6). Briefly, CGNs were plated on 35-mm diameter plastic dishes coated with poly-L-lysine at a density of 2.0×10^6 cells/mL in basal modified Eagle's medium containing 10% fetal bovine serum, 25 mM KCl, 2 mM L-glutamine, penicillin (100 units/mL), streptomycin (100µg/mL) (Life technologies, Inc., Gaithersburg, MD). Cytosine arabinoside (10 µM) was added to the culture medium 24 h after plating to limit the growth of non-neuronal cells. With this protocol, cultures were approximately 95% pure for granule neurons. In general, experiments were performed after 6-7 days in culture.

CGN culture from STAT1 Knockout (KO) mice - STAT1 KO mice and their wild type littermates were obtained commercially from Taconic (Hudson, NY, USA). CGNs from these mice were isolated and cultured essentially as described above.

Cell lysis and immunoblotting - After treatment as described in the Results section, CGN whole-cell lysates or immune complexes of STAT5A or STAT5B were prepared for Western blotting essentially as previously described (8). Protein concentrations were determined by a commercially available protein assay kit (BCA, Thermoscientific, PA, USA) and SDS-polyacrylamide gel electrophoresis was performed

using equal amounts of protein followed by transfer to polyvinylidene difluoride (PVDF) membranes (Amersham Biosciences). Non-specific binding sites were blocked in phosphate buffer saline (PBS) (pH 7.4) containing 0.1% Tween 20 (PBS-T), 1% bovine serum albumin (BSA), and 0.01% sodium azide for 1 h at room temperature (25^{o}C). Membranes were incubated for 1 h in primary antibody diluted in blocking solution. Excess primary antibody was removed by washing the membranes with PBS-T 5 times over 25 min. The membranes were then incubated for 1 h with the appropriate horseradish peroxidase-conjugated secondary antibodies diluted in PBS-T. Excess secondary antibody was removed by washing the membranes with PBS-T 5 times over 25 min. Immunoreactive proteins were detected by enhanced chemiluminescence. Blots shown are representative of a minimum of three independent experiments.

Quantification of apoptosis - After induction of apoptosis, CGNs were fixed in 4% paraformaldehyde for 30 min and nuclei were stained with Hoechst dye (8 µg/mL, final concentration) for 30 min. CGNs containing condensed and/or fragmented nuclei were scored as apoptotic. Typically, approximately 800 cells were quantified from each 35-mm well by randomly counting five 40x fields. Final counts represent data obtained from at least three independent experiments performed in duplicate.

Immunocytochemistry - CGNs were plated at a density of 2.0 x 10^6 cells/mL in 35-mm wells. After ToxB treatment, CGNs were fixed in 4% paraformaldehyde, washed once in PBS, and then permeabilized and blocked in PBS containing 0.2% Triton X-100 and 5% BSA. Primary antibodies were diluted in 2% BSA and 0.2% Triton X-100 in PBS and cells were incubated in primary antibody overnight at 4 ^{o}C. They were subsequently washed 5 times in PBS and then incubated for 1 h with DAPI and either Cy3- or FITC-conjugated secondary antibody diluted in 2% BSA and 0.2% Triton. The cells were washed 5 additional times with PBS before the addition of anti-quench composed of 0.1% *p*-phenylenediamine in 75% glycerol in PBS. Fluorescent images were captured using a 40x water oil immersion objective on a Zeiss Axioplan 2 microscope with a Cooke Sensicam deep-cooled charge-coupled device (CCD) camera and a Slidebook software-analysis program for digital deconvolution (Intelligent Imaging Innovations Inc., Denver, CO, USA).

Preparation of nuclear and cytosolic extracts from CGNs - Nuclear and cytosolic extracts were prepared as described by Li et al., (18). Briefly, CGNs were detached from culture dishes by a cell scraper and centrifuged at 250 x g for 5 min. The cell pellets were washed and homogenized with 15 strokes of a tight-fitting Dounce homogenizer to release nuclei. Next, the homogenate was centrifuged at 14,000 × *g* for 15 sec to pellet the nuclei. The supernatants (cytosolic fractions) were removed, and the pellets were resuspended in a HEPES:glycerol buffer and nuclear proteins were extracted at 4°C for 45 min. Insoluble nuclei were precipitated by centrifugation at 14000 ×*g* for 15 min and the supernatants were dialyzed against a Tris:glycerol buffer for 3 h at 4^{o}C.

Adenovirus preparation and infection -Wild-type STAT5 and dominant-negative STAT5 adenoviral constructs were prepared as described previously (19). CGNs were infected *in vitro* on day 6 with 100 moi (multiplicity of infection) of adenovirus carrying GFP, wild type STAT5, or dominant negative STAT5. At 48 h of infection, cells were treated with 40 ng/mL ToxB. At 72 h of infection, cell lysates were prepared for immunoblot analysis or cells were fixed for immunocytochemistry, as described above.

Chromatin Immunoprecipitation (ChIP) -

ChIP assays were performed according to the manufacturer's protocol using the ChIP assay kit from Active Motif (Carlsbad, CA, USA). CGNs were treated with 40 ng/mL ToxB for 0 and 8 h. Next, DNA associated proteins were cross-linked with formaldehyde. Cross-linked chromatin was extracted, sheared enzymatically, and incubated with a ChIP grade STAT5 antibody overnight at 4°C and protein G-agarose beads. After washing, immune complexes were eluted from the beads, heated to reverse the cross-links, and treated with proteinase K and RNase A to remove proteins and any contaminating RNA. DNA was analyzed by polymerase chain reaction (PCR) using primers provided from SABiosciences that generate a 114-bp product that corresponds to the promoter region of the rat Bcl-xL gene: forward primer, 5′-GAAGCTGACACCAGTG AGTGTCCGAACGGTAAATGCCTACGAAGCTGACACCAGTGAGTG-3′; and reverse primer, 5′ -GTAGGCAT TTACCGTTCGGA-3′. These primers were selected because

they amplify a sequence of DNA that is near two predicted STAT5 binding sites on the promoter region of Bcl-xL variant 1 and variant 2. As a negative control, ChIP reactions were performed as described in the absence of STAT5 antibody followed by PCR. PCR was performed using the following conditions: 1 cycle of 95 °C for 10 min followed by 40 cycles of 95 °C for 15 sec, and 60 °C for 60 sec.

Data analysis - Results represent the mean ± SEM for the number (n) of independent experiments performed. Statistical differences between the means of unpaired sets of data were evaluated by one-way analysis of variance with a *post hoc* Tukey's test. A p-value of < 0.05 was considered statistically significant. Images and immunoblots are representative of at least three independent experiments. For the Ct values reported in Fig. 10A, results represent the mean for four independent experiments and statistical differences were evaluated by a student's t-test.

RESULTS

STAT1 is upregulated in a JAK-dependent manner in CGNs treated with the Rho family GTPase inhibitor ToxB - To evaluate the involvement of Rac in CGN survival, cultures were incubated with *Clostrium difficile* Toxin B. This cytotoxin monoglucosylates a key threonine residue in the switch 1 region of Rho GTPases, thus preventing any interactions with downstream effectors (17,20). We have previously shown that inhibition of the Rho family member, Rac, with ToxB elicits the derepression of a pro-apoptotic JAK/STAT pathway in CGNs (8). However, the specific STAT family protein involved in this pathway has not yet been elucidated. As STAT1 is the most extensively described family member in studies of apoptosis (21-23), we examined its expression following Rac inhibition. CGNs incubated with ToxB for 24 h exhibited a marked increase in the expression of STAT1 (Fig. 1A). Moreover, co-incubation with a small molecule pan-JAK inhibitor (pan-JI; structure shown in Fig. 1B) was sufficient to prevent the induction of STAT1 by ToxB, confirming that the increase in STAT1 is dependent on JAK activation (Fig. 1A).

In addition to provoking apoptosis in a variety of diverse cell types (24-26), activated STAT1 has been shown to play a pro-apoptotic role in neuronal death induced during ischemic brain injury (27). To determine whether derepression of a JAK/STAT1 pathway exerts a similar pro-apoptotic effect in Rac-inhibited neurons, we examined the neuroprotective effects of pan-JI in ToxB-treated CGNs. Examination of nuclei by Hoechst staining revealed increased apoptotic cell death in ToxB-treated CGNs as evidenced by nuclear fragmentation and/or condensation. The effect of ToxB on the morphology of CGN nuclei was significantly attenuated by co-treatment with the pan-JI (Fig. 1D, lower panels). As an additional means of identifying apoptotic cells, we examined caspase-3 activation as cleavage to its active proteolytic fragments is a hallmark of apoptosis and signifies commitment to cell death (28). CGNs treated with ToxB alone exhibited increased activation of caspase-3 and this effect was blocked by pan-JI (Fig. 1D, upper panels). Quantification of apoptosis in CGNs co-incubated with ToxB and pan-JI revealed that the pan-JI conferred significant neuroprotection and effectively reduced apoptosis to control levels (Fig. 1C). Taken together, these data suggest that inhibition of Rac with ToxB results in the activation of a pro-apoptotic JAK/STAT1 signaling pathway in CGNs.

To elucidate the specific JAK family member(s) that induce STAT activation downstream of Rac inhibition in CGNs, we evaluated the protective effects of more targeted JAK inhibitors against ToxB. We found that two specific JAK3 inhibitors (JAK3 Inh and Tofacitinib; Tof) did not confer significant neuroprotection in ToxB-treated CGNs (Fig. 1E). However, we found that the JAK1/2 inhibitor (Ruxolitinib; Rux) modestly protected CGNs from ToxB-mediated apoptosis, although this effect did not quite reach statistical significance. Based on the marked protective effects of the pan-JI (which inhibits JAK1-3 and Tyk2 with similar potency) and our results showing that more targeted inhibition of specific JAK family members (JAK1-3) are not overtly protective, these data suggest a possible contribution of Tyk2 in mediating the apoptosis downstream of ToxB-mediated Rac inhibition in primary CGNs.

STAT1 is not activated by tyrosine phosphorylation nor does it translocate into the nucleus of ToxB-treated CGNs - Next, we examined the phosphorylation status and localization of STAT1 in CGNs exposed to ToxB. In order to translocate into the nucleus and influence gene expression, members of the

STAT family must be activated via tyrosine phosphorylation (29). Whereas total STAT1 expression increased in CGNs treated for 24 h with ToxB, time course experiments performed for up to 24 h did not show significant activation of STAT1 as assessed by tyrosine phosphory-lation (Fig. 2A). Furthermore, using immuno-staining to examine STAT1 localization, we found that STAT1 remained cytosolic and perinuclear in CGNs following ToxB treatment (Fig. 2B). These observations are striking in that they suggest that the observed upregulation of STAT1 expression may not be directly involved in apoptosis following ToxB-mediated inhibition of Rac.

CGNs from STAT1 knockout mice are susceptible to ToxB-induced apoptosis - To definitively establish whether the upregulation of total STAT1 expression, in the absence of enhanced tyrosine phosphorylation or nuclear translocation, is involved in ToxB-mediated apoptosis, we measured the effects of ToxB on primary cultures of CGNs isolated from STAT1 knockout (KO) mice versus their wild type (WT) littermates. CGNs from WT mice demonstrated a marked increase in STAT1 expression following ToxB treatment, whereas CGNs from STAT1 KO mice did not demonstrate any expression of STAT1 in either the absence or presence of ToxB (Fig. 3A), thus confirming effective knock out of STAT1 expression in these mice. Unexpectedly, CGNs from both WT and STAT1 KO mice equally succumbed to apoptosis in response to ToxB treatment (Fig. 3B), while inclusion of the pan-JI was equally neuroprotective for both cell types (Fig. 3C). Collectively, these data indicate that although total STAT1 is upregulated, a different member of the STAT family mediates JAK-dependent apoptosis in Rac-inhibited CGNs.

STAT3 is tyrosine phosphorylated in response to ToxB and this effect is blocked by pan-JI - As our data demonstrate that STAT1 upregulation does not significantly contribute to apoptosis in Rac-inhibited CGNs, we next evaluated the involvement of additional members of the STAT family. Recent evidence suggests that STAT3 mediates β-amyloid-induced apoptosis in mouse cortical neurons (30). To determine if ToxB-targeted inhibition of Rac acts to ultimately activate a similar pro-apoptotic JAK/STAT3 pathway, we analyzed the activation of STAT3 in response to ToxB treatment. Time course experiments demonstrated that STAT3 was tyrosine phosphorylated as early as 6 h after ToxB treatment (Fig. 4A) and inclusion of pan-JI blocked the phosphorylation of STAT3 at both 6 h and 8 h in ToxB-treated CGNs (Fig. 4B).

A reputed STAT3 inhibitor, JSI-124, protects CGNs from ToxB-induced apoptosis - To further define the potential role of STAT3 in the pro-apoptotic pathway activated downstream of Rac inhibition, we examined whether or not the reputed STAT3 inhibitor, JSI-124 (31), exerted a protective effect in ToxB-treated CGNs (Fig. 5A). Following a 24 h incubation period with ToxB alone, many CGNs displayed condensed and/or fragmented nuclei consistent with apoptosis. In contrast, CGNs co-incubated with JSI-124 were essentially completely protected from apoptosis and their nuclei were morphologically similar to control cells (Fig. 5B). Inclusion of JSI-124 reduced CGN apoptosis in the presence of ToxB to approximately 10% (Fig. 5C). These data support a model in which a pro-apoptotic JAK/STAT3 pathway mediates apoptosis in Rac-inhibited CGNs.

Phosphorylated STAT3 does not translocate into the nucleus of CGNs following treatment with ToxB and additional STAT3 inhibitors do not protect CGNs from apoptosis induced by ToxB - To further investigate the role of STAT3 in apoptosis, we examined whether or not pSTAT3 translocates into the nucleus following ToxB treatment. Nuclear fractionation experi-ments demonstrated that although STAT3 was tyrosine phosphorylated, pSTAT3 remained cytosolic following ToxB-targeted inhibition of Rac (Fig. 6A). Furthermore, two additional STAT3 inhibitors, STA-21 and a STAT3 inhibitory peptide, did not protect CGNs from ToxB-induced apoptosis (Figs. 6B, C). These results indicate that STAT3 does not directly regulate apoptosis downstream of Rac inhibition. This finding was particularly surprising as the selective STAT3 inhibitor, JSI-124, exerted a neuroprotective effect in ToxB-treated CGNs. However, further evaluation of the effects of JSI-124 in CGNs revealed that this compound in fact had no significant inhibitory effect on ToxB-induced STAT3 phosphorylation (Fig. 6D). These data suggest that the mechanism by which JSI-124 protects CGNs from apoptosis is unrelated to attenuation of activated STAT3 and may involve a different member of the STAT family.

Tyrosine phosphorylation of STAT5 in response to ToxB in CGNs is blocked by JSI-124 and the putative STAT5 inhibitor, Roscovitine - Recent evidence demonstrates a necessary role for STAT5 in apoptosis induced by oncostatin M in osteosarcoma cells (32). In addition, both STAT5 isoforms have been implicated in the downregulation of the pro-survival Bcl-xL protein in thymocytes (33). Therefore, we next examined STAT5 and found that STAT5 was tyrosine phosphorylated in ToxB-treated CGNs. Interestingly, although blotting for total STAT5 clearly showed the presence of both STAT5A (94 kDa) and STAT5B (92 kDa) in CGNs (Fig. 7A, lower blot), westerns for phospho-STAT5 only indicated a single tyrosine phosphorylated isoform in response to ToxB (Fig. 7A, upper blot). Therefore, we next sought to determine whether STAT5A or STAT5B was phosphory-lated in response to ToxB. To establish which STAT5 isoform was phosphorylated, we compared lysates that were immunoprecipitated for either STAT5A or STAT5B to whole cell lysates and western blotted for total STAT5. Using this approach, we were able to determine where the STAT5A and STAT5B isoforms were detected by immunoblot (Fig. 7B; left panel). Despite efficient immunoprecipitation of each of the STAT5 isoforms from CGNs using isoform-specific antibodies, we were not able to observe tyrosine phosphorylation of either isoform in response to ToxB. However, in whole cell lysates obtained following 8 h of ToxB treatment, we observed a pronounced increase in the tyrosine phosphorylation of the higher molecular weight STAT5A isoform, but not STAT5B, using a phospho-specific antibody to STAT5 (Fig. 7B; right panel). The inability to observe STAT5A tyrosine phosphorylation following immunoprecipitation may reflect the physical association of STAT5A with one or more protein tyrosine phosphatases, anyone of which may be insensitive to the phosphatase inhibitors present in our lysis buffer, as previously described (34,35). Our data are consistent with several previous reports demonstrating that STAT5A and STAT5B can be individually activated in a stimulus- and cell type-specific manner (36-40)

In addition, co-treatment of CGNs with either JSI-124 or the putative STAT5 inhibitor, roscovitine (54), was sufficient to block the tyrosine phosphorylation of STAT5A in response to ToxB (Figs. 7A, B). To further substantiate the involvement of STAT5 in ToxB-treated CGNs, we examined STAT5 phosphorylation and localization by immuno-cytochemistry. In control CGNs, the expression of pSTAT5 detected by immunofluoresence was negligible. In contrast, following incubation of CGNs with ToxB there was a profound increase in the immunoreactivity for pSTAT5 and this transcription factor was principally localized to CGN nuclei (Fig. 7C). Collectively, these data indicate that STAT5 is tyrosine phosphorylated in response to ToxB and localizes to the nucleus under these conditions to modulate gene transcription. Moreover, the tyrosine phosphor-ylation of STAT5 appears to be specific for the STAT5A isoform and is sensitive to inhibition by either JSI-124 or roscovitine.

Roscovitine significantly protects CGNs from ToxB-induced apoptosis - Consistent with STAT5 playing a key role in ToxB-induced apoptosis, CGNs co-treated with ToxB and roscovitine displayed healthy, intact nuclei (Fig. 8A). Quantification of these results show that roscovitine significantly protected CGNs from ToxB-induced apoptosis (Fig. 8B). In addition, ToxB treatment for 24 h resulted in the cleavage of pro-caspase-3 to its active fragments, an effect largely attenuated by roscovitine (Fig. 8C). Generally, roscovitine is used to suppress the cell cycle through inhibition of cyclin-dependent kinases (CDKs) (41). To ensure that the protection conferred by roscovitine was not through CDK suppression, but was a result of STAT5 inhibition, CGNs were also treated with ToxB ± Purvalanol A, a closely related CDK inhibitor. Although remarkably similar in structure, Purvalanol A did not protect CGNs from ToxB-induced apoptosis and in fact, significantly enhanced cell death (Fig. 8D). These results suggest that the neuroprotective effects of roscovitine are unrelated to CDK suppression and are likely due to STAT5 inhibition.

Adenoviral dominant negative STAT5 protects CGNs from ToxB-induced apoptosis -As a more specific approach to definitively establish the pro-apoptotic role of STAT5 following disruption of Rac activity, we examined the neuroprotective effects of a dominant negative mutant of STAT5 containing a C-terminal truncation at residue 713 which removes the entire transcriptional activation domain of STAT5 (Ad-DN STAT5; (42). First, adenovirus expressing either WT STAT5 or DN STAT5 were grown and overexpressed in HEK293AD cells and compared to cells that were infected with the Ad-GFP

control. Infection with Ad-WT STAT5 increased expression of full length STAT5 and Ad-DN STAT5 appeared as a lower molecular weight form of STAT5 (Fig. 9A). Next, we infected CGNs with the Ad-GFP control, WT-STAT5, and DN-STAT5 and observed similar high level expression of the constructs (Fig. 9B). Importantly, none of the adenoviral constructs induced any significant increase in basal apoptosis of CGNs on their own (Fig. 9C). As we have consistently shown, ToxB treatment resulted in condensed and fragmented nuclei indicative of apoptosis. Not unexpectedly, pre-incubation of CGNs with WT STAT5 did not confer neuroprotection from ToxB treatment (Fig. 9E). However, CGNs pre-incubated with Ad-DN STAT5 and subsequently treated with ToxB displayed nuclear morphology strikingly more similar to control CGNs (Fig. 9E). Quantification of apoptosis revealed that inhibiting the transcriptional activity of endogenous STAT5 through overexpression of Ad-DN STAT5 significantly protected CGNs from ToxB-induced apoptosis (Fig. 9D). The protective effect of Ad-DN STAT5 was not as complete as the chemical JAK/STAT inhibitors used previously. This was likely a reflection of the infection efficiency of CGNs which we observed to be approximately 50-60% in cells infected with Ad-GFP. These data highlight a novel pro-apoptotic function for STAT5 downstream of Rac inhibition in primary cerebellar neurons.

STAT5 transcriptionally represses Bcl-xL during ToxB-induced apoptosis - Recent studies suggest that under certain conditions, STAT5 transcriptionally represses pro-survival members of the Bcl-2 family (32,33,43). Disturbances in the ratio of these proteins to their corresponding pro-apoptotic family members can induce apoptosis. The pro-survival members of the Bcl-2 family have an important and well documented role in promoting cell survival through binding and inactivating the pro-apoptotic members of their same family (44). To evaluate if STAT5 similarly represses Bcl-2 family proteins in Rac-inhibited CGNs, we isolated and purified DNA with a ChIP-grade antibody to STAT5 in control CGNs or those treated with ToxB for 8 h. There was no significant difference between STAT5 bound to the promoter region of Bcl-2 in control versus ToxB-treated CGNs (data not shown). In the case of Bcl-xL, the input levels of Bcl-xL promoter DNA amplified from non-immunoprecipitated control and ToxB-treated CGNs were not significantly different. However, the cycle threshold (Ct) values obtained for amplification of the Bcl-xL promoter from STAT5-ChIP samples were significantly lower for ToxB treatment compared to the control, indicating a significant increase in STAT5 binding to the Bcl-xL promoter in Rac-inhibited CGNs (Fig. 10A). Indeed, we report that there was an apparent, though not statistically significant, 9.5±4.1 (n=4) fold increase in STAT5 recruitment to the Bcl-xL promoter in response to ToxB treatment after 8 h (Fig. 10B). Consistent with these data, Bcl-xL expression was downregulated at 16 h and more significantly, at 24 h after ToxB treatment (Fig. 10C). In agreement with a relatively slow mechanism of death due to the transcriptional repression of Bcl-xL, we report that ToxB does not induce caspase-3 activation or significant apoptotic morphology until approximately 16 h of incubation, after STAT5 is bound to the promoter region of Bcl-xL in CGNs (Figs. 10B, C).

DISCUSSION

Several studies have demonstrated a critical role for Rho GTPases (i.e., Rac, Rho, Cdc42) in promoting neuronal survival (45-47). Consistent with these findings, we have previously shown that Rac activity is critical for the survival of primary CGNs (6), and Rac signaling functions to repress a pro-apoptotic JAK/STAT pathway in these neurons (8). Similarly, studies from other groups support a role for the activation of a pro-death JAK/STAT pathway in neurons (48,49). For instance, Takagi et al. (27) reported that STAT1 was phosphorylated on activating tyrosine and serine residues and translocated into neuronal nuclei following ischemic brain injury in mice. Moreover, STAT1 KO mice displayed a decrease in the volume of ischemic brain injury and reduced TUNEL staining when compared to WT mice subjected to middle cerebral artery occlusion. Thus, STAT1 can play a pro-apoptotic role in neurons exposed to ischemic stress. In a similar manner, cortical neurons cultured from STAT1 KO mice showed marked resistance to interferon gamma-stimulated neurotoxicity of the HIV-1 proteins gp120 and Tat (50). A more recent study demonstrated that exposure of SH-SY5Y neuroblastoma cells to interferon beta induced STAT1 tyrosine phosphorylation and caspase-dependent apoptosis (51). Both STAT1

activation and caspase activation were prevented by a JAK inhibitor. Similar to STAT1, STAT3 also has the potential to have a pro-apoptotic effect in neurons under certain conditions. Wan et al. (30) recently showed that a pro-apoptotic Tyk2/STAT3 pathway mediates β-amyloid peptide-induced neuronal death. Specifically, siRNA knockdown of STAT3 protected PC12 cells from β-amyloid and a STAT3 inhibitory peptide protected cultured cortical neurons. Finally, cortical neurons isolated from Tyk2 null mice were significantly less sensitive than WT neurons to β-amyloid-induced apoptosis. Collectively, these studies demonstrate that both STAT1 and STAT3 have the potential of acting as pro-apoptotic mediators in neurons under specific pathological conditions. In contrast to these previous reports, we find that although total STAT1 levels are upregulated and STAT3 is activated via tyrosine phosphorylation in response to ToxB, neither transcription factor is responsible for the neuronal apoptosis induced in CGNs by inhibition of Rac function.

Instead, we report that ToxB induces the enhanced tyrosine phosphorylation of STAT5 which subsequently translocates into the nucleus of CGNs. Interestingly, we found that the phosphorylation of STAT5 was prevented by the reputed STAT3 inhibitor, JSI-124. This finding is perhaps not surprising given that JSI-124 has been reported to exert effects outside of STAT3 inhibition (52). In fact, this compound was recently shown to inhibit the neuroprotective effects of growth hormone against glutamate-induced toxicity in hippocampal neurons, an effect which is dependent on STAT5 activity (53). In addition to the neuroprotective effects of JSI-124, we report that roscovitine similarly inhibits STAT5 phosphorylation induced by ToxB and protects CGNs against ToxB-targeted Rac inhibition. The effects of roscovitine were dissociated from its effects as a CDK inhibitor since the similarly structured compound, Purvalanol A, did not protect CGNs from ToxB. Our data with roscovitine are consistent with a previous study showing its ability to suppress STAT5 activation in a leukemia cell line (54). Finally, we show that adenoviral infection with a dominant negative mutant of STAT5, but not WT STAT5, significantly protects CGNs from Rac inhibition with ToxB. To our knowledge, these findings are novel in that they are the first to identify a pro-apoptotic function for STAT5 in neurons.

Our data indicate that of the two STAT5 isoforms, only STAT5A is activated via phosphorylation in CGNs exposed to ToxB-mediated Rac blockage. Although the two isoforms are highly homologous, this is consistent with several previous reports which have revealed isoform-specific STAT5 activation. Similar to our results in CGNs, JAK/STAT signaling has been shown to induce caspase-dependent apoptosis in response to granulocyte-macrophage colony-stimulating factor (GM-CSF) in OCIM2 acute myeloid leukemia cells (36). However, while GM-CSF has been shown to preferentially activate STAT5A in human monocytes (37), this factor was shown to induce specific STAT5B signaling in human neutrophils (38). In a similar manner, insulin was demonstrated to activate STAT5B, but not STAT5A, in Kym-1 rhabdomyosarcoma cells (39). Furthermore, targeted gene disruptions of either STAT5A or STAT5B in mice have shown functional differences *in vivo*. For example, deletion of STAT5A disrupts prolactin-derived mammary gland maturation while disruption of STAT5B diminishes growth hormone effects on hepatic function and body mass in male mice (40). Thus, our data are consistent with several previous reports highlighting isoform-specific activation and functions of STAT5.

STAT5 is activated by many diverse cytokines and growth factors and it is well established that this transcription factor has an important role throughout the body. Although few studies have examined the role of STAT5 in the central nervous system, the majority of reports are paradoxical to our present study and suggest that STAT5 chiefly exerts a pro-survival effect in neurons. For example, STAT5 is required in conjunction with Akt in order to mediate the neurotrophic and neuroprotective effects of both growth hormone in hippocampal neurons (53) and erythropoietin in differentiated neuroblastoma cells (55). Furthermore, STAT5 was shown to elicit a pro-survival effect via induction of Bcl-2 and Bcl-xL in neural progenitor cells subjected to apoptotic stimulation (56). Thus, the relatively few studies conducted on STAT5 in neuronal models indicate that it mainly functions to transmit pro-survival signals. Yet, critical studies in non-neuronal cells suggest that the downstream effects of STAT5 are much more complex. STAT5 sensitizes osteosarcoma cells to apoptosis following treatment with oncostatin M (32). Moreover,

in a mouse model of familial ALS, a JAK3 inhibitor was shown to extend the lifespan of mutant mice when compared to those that did not receive the inhibitor. While the effects of this inhibitor on the activation of specific STAT family members was not evaluated in this particular study, JAK3 has been shown to activate STAT5 on various accounts (57-59). In evaluating various JAK isoform-selective inhibitors, we did not observe any significant inhibition of ToxB-induced apoptosis in CGNs except with a pan-JI. Thus, our data suggest a possible contribution of Tyk2 or multiple JAK isoforms in the apoptosis of neurons subjected to Rac inhibition. In conjunction with our present findings, these previous studies suggest that STAT5 functions in a cell-type and stimulus-specific manner and the specific role of JAK/STAT5 in the central nervous system and in particular, with respect to neuronal survival, is likely determined by many factors.

While we have identified Rac as a repressor of a pro-apoptotic JAK/STAT5 pathway, the mechanism of STAT5 activation following Rac inhibition remains incompletely understood. Suppressors of cytokine signaling (SOCS) exist as endogenous STAT inhibitors (60,61) and previous evidence suggests that SOCS protein expression can be regulated by ERK (62,63). This is consistent with our previous finding that a pro-survival MEK/ERK pathway functions downstream of Rac GTPase to actively repress pro-apoptotic JAK/STAT signaling in healthy CGNs (8). Whether SOCS proteins are indeed mediators of the Rac-dependent repression of pro-apoptotic JAK/STAT signaling in neurons remains to be investigated.

In agreement with our work identifying a pro-apoptotic JAK/STAT5 pathway in CGNs, recent examination of the genetic targets of STAT5 demonstrate transcriptional regulation of pro-survival members of the Bcl-2 family. For example, STAT5 has been shown to negatively regulate the levels of Bcl-2 in osteosarcoma cells sensitized to undergo apoptosis (32). Similarly, both STAT5 isoforms were shown to bind to the promoter region of Bcl-x, a gene which is transcribed into pro-survival Bcl-xL and pro-apoptotic Bcl-extra short (Bcl-xS) (33,43,64). Therefore, it was of interest to determine if Bcl-2 and/or Bcl-xL were transcriptional targets of STAT5 in CGNs subjected to Rac inhibition with ToxB. Our ChIP data show that STAT5 is recruited to the Bcl-xL promoter in ToxB-treated CGNs. These results suggest that STAT5 may transcriptionally repress Bcl-xL to tip the delicate balance between pro-survival and pro-apoptotic Bcl-2 proteins towards apoptosis. Consistent with this interpretation, we observe caspase-3 activation and classical apoptotic morphology subsequent to downregulation of Bcl-xL protein levels. While we show that STAT5 binding to the promoter region of Bcl-xL increases in response to Rac inhibition, an alternative mechanism by which STAT5 may mediate transcriptional repression of Bcl-2 family proteins in the nucleus is through competitive binding to the transcriptional co-activator p300/CREB binding protein (CBP) (65,66). At the present time, we cannot exclude this as a possible mechanism of STAT5-dependent transcriptional repression of Bcl-xL during Rac inhibition.

Another potential mechanism by which STAT5 has been proposed to repress Bcl-xL transcription involves a cooperative interaction with the glucocorticoid receptor (GR). A recent report found that glucocorticoid treatment in lymphoid cells inhibited the transcription of Bcl-xL and decreased the ratio of Bcl-xL to the pro-apoptotic Bcl-xS in a STAT5B-dependent manner to induce apoptosis (13). Conversely, another report found that the GR can interact with STAT5 to upregulate Bcl-xL as part of a pro-survival pathway activated by the GR agonist, methylprednisolone, in oligodendro-cytes (67). Given the evidence suggesting that the GR can act in a cooperative manner with STAT5 to regulate the transcription of Bcl-xL, we sought to determine whether or not the GR was involved in STAT5A-mediated apoptotic signaling in CGNs subjected to ToxB treatment. In CGNs exposed to ToxB, the GR antagonist, mifepristone, provided no significant protection indicating that the STAT5-dependent effects on Bcl-xL transcription are likely GR-independent in this cell system (data not shown).

In summary, we show that ToxB-induced inactivation of Rac GTPase results in the derepression of a novel pro-apoptotic JAK/ STAT5 pathway. Although STAT1 was induced and STAT3 was phosphorylated following ToxB treatment, neither protein was responsible for inducing apoptosis of CGNs downstream of Rac inhibition. Rather, our data support a model in which ToxB-induced Rac inhibition in CGNs activates a novel pro-apoptotic JAK/STAT5 pathway which, following STAT5A phosphory-lation and translocation to the nucleus, results in the transcriptional repression of pro-survival

Bcl-xL and subsequent activation of caspase-3 and apoptosis. To our knowledge, our findings are novel in that they are the first to demonstrate a pro-apoptotic function for a JAK/STAT5 pathway in neurons.

REFERENCES

1. Olson, M. F., Ashworth, A., and Hall, A. (1995) *Science* **269**, 1270-1272
2. Hill, C. S., Wynne, J., and Treisman, R. (1995) *Cell* **81**, 1159-1170
3. Clark, E. A., King, W. G., Brugge, J. S., Symons, M., and Hynes, R. O. (1998) *J Cell Biol* **142**, 573-586
4. Fukata, M., Kuroda, S., Nakagawa, M., Kawajiri, A., Itoh, N., Shoji, I., Matsuura, Y., Yonehara, S., Fujisawa, H., Kikuchi, A., and Kaibuchi, K. (1999) *J Biol Chem* **274**, 26044-26050
5. Tanaka, T., Tatsuno, I., Uchida, D., Moroo, I., Morio, H., Nakamura, S., Noguchi, Y., Yasuda, T., Kitagawa, M., Saito, Y., and Hirai, A. (2000) *J Neurosci* **20**, 2852-2859
6. Linseman, D. A., Laessig, T., Meintzer, M. K., McClure, M., Barth, H., Aktories, K., and Heidenreich, K. A. (2001) *J Biol Chem* **276**(42), 39123-39131
7. Jacquier, A., Buhler, E., Schafer, M. K., Bohl, D., Blanchard, S., Beclin, C., and Haase, G. (2006) *Ann Neurol* **60**, 105-117
8. Loucks, F. A., Le, S. S., Zimmermann, A. K., Ryan, K. R., Barth, H., Aktories, K., and Linseman, D. A. (2006) *J Neurochem* **97,** 957-967
9. Igaz, P., Toth, S., and Falus, A. (2001) *Inflamm Res* **50**, 435-441
10. Yamauchi-Takihara, K., and Kishimoto, T. (2000) *Int J Exp Pathol* **81**, 1-16
11. Watson, C. J., and Miller, W. R. (1995) *Br J Cancer* **71**, 840-844
12. Kim, W. H., Hong, F., Radaeva, S., Jaruga, B., Fan, S., and Gao, B. (2003) *Am J Physiol Gastrointest Liver Physiol* **285**, G761-768
13. Rocha-Viegas, L., Vicent, G. P., Baranao, J. L., Beato, M., and Pecci, A. (2006) *J Biol Chem* **281**, 33959-33970
14. D'Mello, S. R., Galli, C., Ciotti, T., and Calissano, P. (1993) *Proc Natl Acad Sci U S A* **90**, 10989-10993
15. Contestabile, A. (2002) *Cerebellum* **1**, 41-55
16. Vaudry, D., Falluel-Morel, A., Basille, M., Pamantung, T. F., Fontaine, M., Fournier, A., Vaudry, H., and Gonzalez, B. J. (2003) *J Neurosci Res* **72**, 303-316
17. Just, I., Selzer, J., Wilm, M., von Eichel-Streiber, C., Mann, M., and Aktories, K. (1995) *Nature* **375**, 500-503
18. Li, M., Linseman, D. A., Allen, M. P., Meintzer, M. K., Wang, X., Laessig, T., Wierman, M. E., and Heidenreich, K. A. (2001) *J Neurosci* **21**, 6544-6552

19. Ahonen, T. J., Xie, J., LeBaron, M. J., Zhu, J., Nurmi, M., Alanen, K., Rui, H., and Nevalainen, M. T. (2003) *J Biol Chem* **278**, 27287-27292
20. Jank, T., and Aktories, K. (2008) *Trends Microbiol* **16**, 222-229
21. Sahni, M., Raz, R., Coffin, J. D., Levy, D., and Basilico, C. (2001) *Development* **128**, 2119-2129
22. Stephanou, A., and Latchman, D. S. (2003) *Int J Exp Pathol* **84**, 239-244
23. Sironi, J. J., and Ouchi, T. (2004) *J Biol Chem* **279**, 4066-4074
24. Thomas, M., Finnegan, C. E., Rogers, K. M., Purcell, J. W., Trimble, A., Johnston, P. G., and Boland, M. P. (2004) *Cancer Res* **64**, 8357-8364
25. Kaganoi, J., Watanabe, G., Okabe, M., Nagatani, S., Kawabe, A., Shimada, Y., Imamura, M., and Sakai, Y. (2007) *Ann Surg Oncol* **14**, 1405-1415
26. Soond, S. M., Carroll, C., Townsend, P. A., Sayan, E., Melino, G., Behrmann, I., Knight, R. A., Latchman, D. S., and Stephanou, A. (2007) *FEBS Lett* **581**, 1217-1226
27. Takagi, Y., Harada, J., Chiarugi, A., and Moskowitz, M. A. (2002) *J Cereb Blood Flow Metab* **22**, 1311-1318
28. Porter, A. G., and Janicke, R. U. (1999) *Cell Death Differ* **6**, 99-104
29. Rawlings, J. S., Rosler, K. M., and Harrison, D. A. (2004) *J Cell Sci* **117**, 1281-1283
30. Wan, J., Fu, A. K., Ip, F. C., Ng, H. K., Hugon, J., Page, G., Wang, J. H., Lai, K. O., Wu, Z., and Ip, N. Y. *J Neurosci* **30**, 6873-6881
31. Blaskovich, M. A., Sun, J., Cantor, A., Turkson, J., Jove, R., and Sebti, S. M. (2003) *Cancer Res* **63**, 1270-1279
32. Chipoy, C., Brounais, B., Trichet, V., Battaglia, S., Berreur, M., Oliver, L., Juin, P., Redini, F., Heymann, D., and Blanchard, F. (2007) *Oncogene* **26**, 6653-6664
33. Nelson, E. A., Walker, S. R., Alvarez, J. V., and Frank, D. A. (2004) *J Biol Chem* **279**, 54724-54730
34. Chughtai, N., Schimchowitsch, S., Lebrun, J. J., and Ali, S. (2002) *J Biol Chem* **277**, 31107-31114
35. Rigacci, S., Talini, D., and Berti, A. (2003) *Biochem Biophys Res Commun* **312**, 360-366
36. Faderl, S., Harris, D., Van, Q., Kantarjian, H. M., Talpaz, M., and Estrov, Z. (2003) *Blood* **102**, 630-637
37. Rosen, R. L., Winestock, K. D., Chen, G., Liu, X., Hennighausen, L., and Finbloom, D. S. (1996) *Blood* **88**, 1206-1214
38. al-Shami, A., Bourgoin, S. G., and Naccache, P. H. (1997) *Blood* **89**, 1035-1044
39. Storz, P., Doppler, H., Pfizenmaier, K., and Muller, G. (1999) *FEBS Lett* **464**, 159-163
40. Grimley, P. M., Dong, F., and Rui, H. (1999) *Cytokine Growth Factor Rev* **10**, 131-157
41. Edamatsu, H., Gau, C. L., Nemoto, T., Guo, L., and Tamanoi, F. (2000) *Oncogene* **19**, 3059-3068
42. Wang, D., Stravopodis, D., Teglund, S., Kitazawa, J., and Ihle, J. N. (1996) *Mol Cell Biol* **16**, 6141-6148
43. Moucadel, V., and Constantinescu, S. N. (2005) *J Biol Chem* **280**, 13364-13373
44. Korsmeyer, S. J., Shutter, J. R., Veis, D. J., Merry, D. E., and Oltvai, Z. N. (1993) *Semin Cancer Biol* **4**, 327-332
45. Kobayashi, K., Takahashi, M., Matsushita, N., Miyazaki, J., Koike, M., Yaginuma, H., Osumi, N., Kaibuchi, K., and Kobayashi, K. (2004) *J Neurosci* **24**, 3480-3488
46. Kanekura, K., Hashimoto, Y., Kita, Y., Sasabe, J., Aiso, S., Nishimoto, I., and Matsuoka, M. (2005) *J Biol Chem* **280**, 4532-4543
47. Cheung, Z. H., Chin, W. H., Chen, Y., Ng, Y. P., and Ip, N. Y. (2007) *PLoS Biol* **5**, e63
48. Mäkelä, J., Koivuniemi, R., Korhonen, L., and Lindholm, D. (2010) *PLoS One* **14**, e11091
49. Colodner, K. J., and Feany, M. B. *J Neurosci* **30**, 16102-16113
50. Giunta, B., Obregon, D., Hou, H., Zeng, J., Sun, N., Nikolic, V., Ehrhart, J., Shytle, D., Fernandez, F., and Tan, J. (2006) *Brain Res* **1123**, 216-225
51. Dedoni, S., Olianas, M. C., and Onali, P. *J Neurochem* **115**, 1421-1433

52. Graness, A., Poli, V., and Goppelt-Struebe, M. (2006) *Biochem Pharmacol* **72**, 32-41
53. Byts, N., Samoylenko, A., Fasshauer, T., Ivanisevic, M., Hennighausen, L., Ehrenreich, H., and Siren, A. L. (2008) *Cell Death Differ* **15**, 783-792
54. Mohapatra, S., Chu, B., Wei, S., Djeu, J., Epling-Burnette, P. K., Loughran, T., Jove, R., and Pledger, W. J. (2003) *Cancer Res* **63**, 8523-8530
55. Um, M., and Lodish, H. F. (2006) *J Biol Chem* **281**, 5648-5656
56. Choi, J. K., Kim, K. H., Park, H., Park, S. R., and Choi, B. H. *Apoptosis* **16**, 127-134
57. Bingisser, R. M., Tilbrook, P. A., Holt, P. G., and Kees, U. R. (1998) *J Immunol* **160**, 5729-5734
58. Cavalcanti, E., Gigante, M., Mancini, V., Battaglia, M., Ditonno, P., Capobianco, C., Cincione, R. I., Selvaggi, F. P., Herr, W., Storkus, W. J., Gesualdo, L., and Ranieri, E. *J Biomed Biotechnol* **2010**, 935764
59. Martin, P., Gomez, M., Lamana, A., Cruz-Adalia, A., Ramirez-Huesca, M., Ursa, M. A., Yanez-Mo, M., and Sanchez-Madrid, F. *Mol Cell Biol* **30**, 4877-4889
60. Krebs, D. L., and Hilton, D. J. (2001) *Stem Cells* **19**, 378-387
61. Cooney, R. N. (2002) *Shock* **17**, 83-90
62. Terstegen, L., Gatsios, P., Bode, J. G., Schaper, F., Heinrich, P. C., and Graeve, L. (2000) *J Biol Chem* **275**, 18810-18817
63. Borland, G., Bird, R. J., Palmer, T. M., and Yarwood, S. J. (2009) *J Biol Chem* **284**, 17391-17403
64. Boise, L. H., Gonzalez-Garcia, M., Postema, C. E., Ding, L., Lindsten, T., Turka, L. A., Mao, X., Nunez, G., and Thompson, C. B. (1993) *Cell* **74**, 597-608
65. Zhu, M., John, S., Berg, M., and Leonard, W. J. (1999) *Cell* **96**, 121-130
66. Zhang, J., Yamada, O., Kawagishi, K., Araki, H., Yamaoka, S., Hattori, T., and SShimotohno, K. (2008) *Virology* **379**, 306-313
67. Xu, J., Chen, S., Chen, H., Xiao, Q., Hsu, C. Y., Michael, D., and Bao, J. (2009) *J Neurosci* **29**, 2022-2026

ACKNOWLEDGMENTS

This work was funded by a Merit Review award from the Department of Veterans Affairs (to D.A.L.) and R01 NS062766 from the National Institute of Neurological Disorders and Stroke (to D.A.L.).

FOOTNOTES

[1]The abbreviations used are: CGNs, cerebellar granule neurons; ToxB, *Clostridium difficile* Toxin B; JAK, Janus kinase; STAT, signal transducer and activator of transcription; GEF, guanine nucleotide exchange factor; CHIP; chromatin immunoprecipitation; PAK, p21-activated kinase; MEK, MAP kinase kinase; ERK, extracellular signal-regulated kinase; KO, knockout; SDS-PAGE, sodium dodecylsulfate-polyacrylamide gel electrophoresis; PVFD, polyvinylidene difluoride; PBS; phosphate buffered saline; WT, wild type; pan-JI; pan-JAK inhibitor; pSTAT3, phosphorylated STAT3; pSTAT5, phosphorylated STAT5, CDKs, cyclin-dependent kinases; Ad, adenoviral; SOCS, suppressors of cytokine signaling; Con, control; Cyto, cytosolic; NS, non-specific; IB, immunoblotted; Endo; endogenous; Trunc, truncated; Ct, cycle threshold; O.D., optical density

FIGURE LEGENDS

Figure 1. STAT1 is upregulated in a JAK-dependent manner during CGN apoptosis induced by the Rho family GTPase inhibitor, ToxB. A. CGNs were incubated for 24 h in complete medium containing 25 mM KCl and serum (Con medium) ± C. difficile ToxinB (ToxB; 40 ng/mL), or ToxB + pan-JAK inhibitor (pan-JI; 1 μM). Cells were then lysed and proteins were resolved by SDS-PAGE and

transferred to PVDF membranes. The membrane was probed with an antibody against STAT1. STAT1 expression was upregulated when treated with ToxB and this effect was blocked by pan-JI. B. Molecular structure of pan-JI. C. Quantification of apoptosis in CGNs incubated for 24 h as described in (A). ** $p<0.01$ compared to Con; †† $p<0.01$ compared to ToxB. D. CGNs were incubated for 24 h as described in (A). Following incubation, cells were incubated with a polyclonal antibody against active caspase-3 (shown in red), a monoclonal antibody against β-tubulin (shown in green), and nuclei were stained with DAPI (shown in blue). Lower panels show decolorized DAPI staining of nuclei for clarity. CGNs incubated with ToxB exhibited many condensed and/or fragmented nuclei and displayed increased immunoreactivity for active caspase-3. CGNs co-incubated with pan-JI were significantly protected from apoptosis and displayed nuclear morphology similar to controls. Scale bar = 10 μM. E. CGNs were incubated for 24 h in con medium ± ToxB (40 ng/mL), or ToxB + JAK3 Inhibitor (JAK3 Inh; 100 μM); Ruxolitinib (Rux; 10 μM); or Tofacitinib (Tof; 10 μM). Following incubation, cells were fixed with 4% paraformaldehyde and the nuclei were stained with Hoechst dye. Apoptotic cells were scored as those with condensed and/or fragmented nuclei.

Figure 2. STAT1 does not display increased tyrosine phosphorylation nor does it translocate into the nucleus of ToxB-treated CGNs. A. A 24 h time course of ToxB treatment (40 ng/mL) was performed in CGNs. Cell lysates were resolved by SDS-PAGE and proteins transferred to PVDF membranes. The blots were probed with antibodies against pSTAT1(Y701) and STAT1. Little-to-no increase in the tyrosine phosphorylation of STAT1 was observed in CGNs subjected to ToxB for up to 24 h. B. CGNs were incubated with Con medium ± ToxB (40 ng/mL) for 8 h. Cells were fixed and their nuclei stained with DAPI. A primary antibody against pSTAT1 (Y701) and a Cy3-conjugated secondary antibody were used to visualize pSTAT1. Incubation of CGNs with ToxB did not result in translocation of pSTAT1 into the nucleus. Scale bar = 10 μM.

Figure 3. CGNs from STAT1 knockout and wild type mice are equally susceptible to ToxB-induced apoptosis. A. CGNs from wild-type (WT) and STAT1 knock out (KO) mice were treated for 0 h, 24h, or 48 h with ToxB (40 ng/mL). Cell lysates were resolved by SDS-PAGE and proteins were transferred to PVDF membranes. The blot was probed with a primary antibody against STAT1. Western blot shows induced expression of STAT1 in WT CGNs after treatment with ToxB. B.WT and STAT1 KO CGNs were incubated for 48 h in Con medium ± ToxB (40 ng/mL), or with ToxB + pan-JI (1 μM). Cells were fixed and nuclei were stained with Hoechst. Both WT and KO cells treated with ToxB displayed condensed and/or fragmented nuclear morphology. WT and KO CGNs co-incubated with pan-JI exhibited nuclear morphologies similar to those of con cells. Scale bar = 10 μM. C. Quantification of apoptosis in CGNs incubated for 24 h or 48 h with Con medium ± ToxB (40 ng/mL), or ToxB + pan-JI (1 μM). STAT1 KO cells succumbed to apoptosis as readily as WT CGNs after treatment with ToxB. When co-incubated with pan-JI, STAT1 KO and WT CGNs showed similar protection from ToxB. ** $p<0.01$ compared to Con; †† $p<0.01$ compared to ToxB.

Figure 4. STAT3 is tyrosine phosphorylated in response to ToxB in CGNs and this effect is blocked by pan-JI. A. CGNs were incubated for various periods of time up to 8 h with ToxB in Con medium. Cells were lysed and proteins were resolved by SDS-PAGE and transferred to PVDF membranes. The blot was probed with antibodies against pSTAT3 (Y705) or STAT3. The expression of pSTAT3 increased in response to ToxB. B. CGNs were incubated for 6 h or 8 h in Con medium ± ToxB (40 ng/mL), or ToxB + pan-JI (1 μM). Cell lysates were resolved by SDS-PAGE and proteins were transferred to PVDF membranes. The blot was probed with antibodies against pSTAT3 (Y705) or STAT3. The pan-JI inhibitor blocked ToxB-induced STAT3 phosphorylation.

Figure 5. A reputed STAT3 inhibitor, JSI-124, protects CGNs from ToxB-induced apoptosis. A. Molecular structure of JSI-124. B. CGNs were incubated for 24 h in Con medium ± ToxB (40 ng/mL), or ToxB + JSI-124 (5 μM). Cells were fixed and their nuclei stained with Hoechst dye. CGNs treated with

ToxB exhibited significantly more condensed and/or fragmented nuclei than Con CGNs. CGNs co-incubated with JSI-124 were significantly protected from apoptosis and their nuclei were morphologically similar to Con cells. Scale bar = 10 μM. C. Quantification of apoptosis in CGNs treated with ToxB or ± JSI-124. Values are mean ± SEM. JSI-124 significantly protected CGNs from ToxB-induced apoptosis. ** $p<0.01$ compared to Con; †† $p<0.01$ compared to ToxB.

Figure 6. Phosphorylated STAT3 does not translocate into the nucleus of CGNs following treatment with ToxB and additional STAT3 inhibitors do not protect CGNs from apoptosis. A. CGNs were incubated in Con medium ± ToxB (40 ng/mL) for 8 h. Following incubation, the cells were fractionated into nuclear and cytosolic (cyto) fractions as described in the Experimental Procedures. A monoclonal antibody against pSTAT3 (Y705) was used for Western Blotting. pSTAT3 did not translocate into the nucleus following treatment with ToxB. The purity of the nuclear fractions was verified by immunoblotting for LAP-2. B. CGNs were incubated for 24 h in Con medium ± ToxB (40 ng/mL) or ToxB + STA-21 (20 μM). Cells were fixed and nuclei were stained with Hoechst dye to quantify apoptosis. STA-21 did not protect CGNs from ToxB-induced apoptosis. Results shown are mean ± range (n=2). C. CGNs were incubated for 24 h in Con medium ± ToxB (40 ng/mL) or ToxB + STAT3 inhibitory peptide (100 μM). Cells were fixed and nuclei were stained with Hoechst dye to quantify apoptosis. STAT3 inhibitory peptide did not protect CGNs from ToxB-induced apoptosis. Results shown are mean ± range (n=2). D. CGNs were incubated for 24 h in Con medium ± ToxB (40 ng/mL), JSI-124 (5 μM), or ToxB + JSI-124. The cells were lysed and proteins were separated by SDS-PAGE and transferred to PVDF membranes. Blots were probed for pSTAT3 (Y705). ToxB increased the expression of pSTAT3. This effect was not blocked by co-incubation with JSI-124. NS = non-specific band shown to indicate equal protein loading.

Figure 7. STAT5A shows enhanced tyrosine phosphorylation in response to ToxB in CGNs which is blocked by JSI-124 and the STAT5 inhibitor, roscovitine. A. CGNs were incubated in Con medium ± ToxB (40 ng/mL) or ToxB + JSI-124 (JSI; 5 μM) for 24 h. Cells were lysed, proteins were resolved by SDS-PAGE and transferred to PVDF membranes. Blots were probed for pSTAT5 (Y694) and total STAT5. STAT5 was phosphorylated in response to ToxB and this effect was blocked by JSI-124. B. CGNs were incubated in Con medium ± ToxB (40 ng/mL) or ToxB + roscovitine (Rosc; 30 μM) for 24 h. Following incubation, cells were lysed and immunoprecipitated (IP; right panel) for either total STAT5A or STAT5B. IP'd proteins and a lane containing the whole cell lysate (WCL) were resolved by SDS-PAGE and transferred to PVDF membranes. Blots were probed for total STAT5. On the left panel, proteins were lysed following a 24 h incubation period and resolved by SDS-PAGE. Next, proteins were transferred to PVDF membranes. Blots were probed for pSTAT5 (Y694) and total STAT5. STAT5 was phosphorylated in response to ToxB and this effect was blocked by roscovitine. NS = non-specific; band shown to indicate equal protein loading 5A = STAT5A; 5B = STAT5B. C. CGNs were incubated in Con medium ± ToxB (40 ng/mL) for 24 h. Cells were fixed and incubated with a polyclonal antibody against pSTAT5 (Y694; shown in green). Nuclei were stained with DAPI (shown in blue). pSTAT5 translocates into the nucleus in response to ToxB. Scale bar = 10 μM.

Figure 8. Roscovitine significantly protects CGNs from ToxB-induced apoptosis. A. CGNs were incubated for 24 h in Con medium ± ToxB (40 ng/mL) or ToxB + Roscovitine (Rosc; 30 μM). Following incubation, cells were fixed and the nuclei were stained with Hoechst dye. Scale bar = 10 μM. B. Quantification of apoptosis in CGNs treated with ToxB alone or co-treated with Roscovitine. Values are mean ± SEM (n=5). Roscovitine significantly protected CGNs from ToxB-induced apoptosis. ** $p<0.01$ compared to Con; †† $p<0.01$ compared to ToxB. C. CGNs were as described in (A) and lysed. Proteins were separated by SDS-PAGE and transferred to PVDF membranes. The membrane was immunoblotted (IB) for caspase-3. Roscovitine blocked the ToxB-induced processing of caspase-3 to its active fragments. fl = full length. D. CGNs were incubated for 24 h in Con medium ± ToxB (40 ng/mL) or

ToxB + Purvalanol A (30 μM). Following incubation, cells were fixed with 4% paraformaldehyde and the nuclei were stained with Hoechst dye. Purvalanol A did not protect CGNs from ToxB-induced apoptosis.

Figure 9. Adenoviral dominant negative STAT5 protects CGNs from ToxB-induced apoptosis. A. HEK 293 AD cells were infected for 48 h with an adenovirus carrying GFP (Ad-GFP), wild type STAT5 (Ad-WT STAT5), or dominant negative STAT5 (Ad-DN STAT5). Cell lysates were separated by SDS-PAGE, transferred to PVDF membranes, and immunoblotted (IB) for STAT5 expression. There was a marked increase in STAT5 expression in HEK cells infected with either Ad-WT or Ad-DN STAT5. Endo, endogenous; trunc; truncated. B. CGNs were infected for 48 h with the same adenoviruses as described in (A) and cell lysates were probed for STAT5 expression. C. CGNs were incubated for 48 h with adenoviruses as described above. The cells were fixed and the nuclei were stained with Hoechst. Apoptotic cells were scored as those with condensed and/or fragmented nuclei. There was no significant difference in basal apoptosis in CGNs infected with Ad-GFP, Ad-WT STAT5, or Ad-DN STAT5. D. CGNs were infected for 48 h with either Ad-WT STAT5 or Ad-DN STAT5. After the initial 24 h of incubation, each experimental condition was treated ± ToxB (40 ng/mL) for 24 h. At the end of the incubation, cells were fixed and nuclei were stained with DAPI. Apoptotic cells were scored as those with condensed and/or fragmented nuclei. The fold change in apoptosis for ToxB-treated cells vs. Con cells was quantified. CGNs incubated with dominant negative STAT5 were protected from ToxB-induced apoptosis. Data shown represent the mean ± SEM for n=3 experiments. ** $p < 0.01$ vs. WT STAT5. E. CGNs were incubated as describe in (D). Cells were then fixed and nuclei were stained with Hoechst dye. Images shown are representative of 3 independent experiments. Scale bar = 10 μM.

Figure 10. STAT5 transcriptionally represses Bcl-xL during ToxB-induced apoptosis. STAT5 transcriptionally represses Bcl-xL during ToxB-induced apoptosis. A. CGNs were incubated in Con medium ± ToxB (40 ng/mL) for 8 h. As a control for ChIP experiments ("Input"), ChIP-qPCR was performed as described under "Experimental Procedures" in the absence of the STAT5 antibody to determine the total concentration of input Bcl-xL promoter DNA. The graph shows the mean ± SEM of the results of four independent experiments. The concentration of input DNA did not differ significantly between the Con and ToxB samples. ChIP: STAT5 - CGNs were incubated in Con medium ± ToxB (40 ng/mL) for 8 h. The relative binding of STAT5 to the Bcl-xL promoter was assessed via ChIP-qPCR analysis as described under "Experimental Procedures." The graph shows the mean ± SEM of the results for four independent experiments. STAT5 binding to the Bcl-xL promoter was significantly increased in response to ToxB treatment for 8 h. *$p < 0.05$ vs. Con evaluated by a two-tailed student's t-test. B. The fold enrichment of STAT5 recruitment to the Bcl-xL promoter was quantified from the Ct Value. STAT5 binding to the promoter region of Bcl-xL increased 9.5 + 4.1 in response to 8 h ToxB treatment, although not statistically significant. C. CGNs were incubated for 0, 16, and 24 h with ToxB (40 ng/mL). Cells were then lysed and proteins were resolved by SDS-PAGE and transferred to PVDF membranes. The membrane was probed with an antibody against Bcl-xL. Subsequently, the blot was stripped and reprobed for active caspase-3 and actin (loading control). Bcl-xL expression decreased in response to ToxB and active caspase-3 expression increased. The values above the Bcl-xL blot represent optical densities (O.D) of the Bcl-xL expression. The normalized O.D. for the time "0" control was set to 1.0.

Figure 1

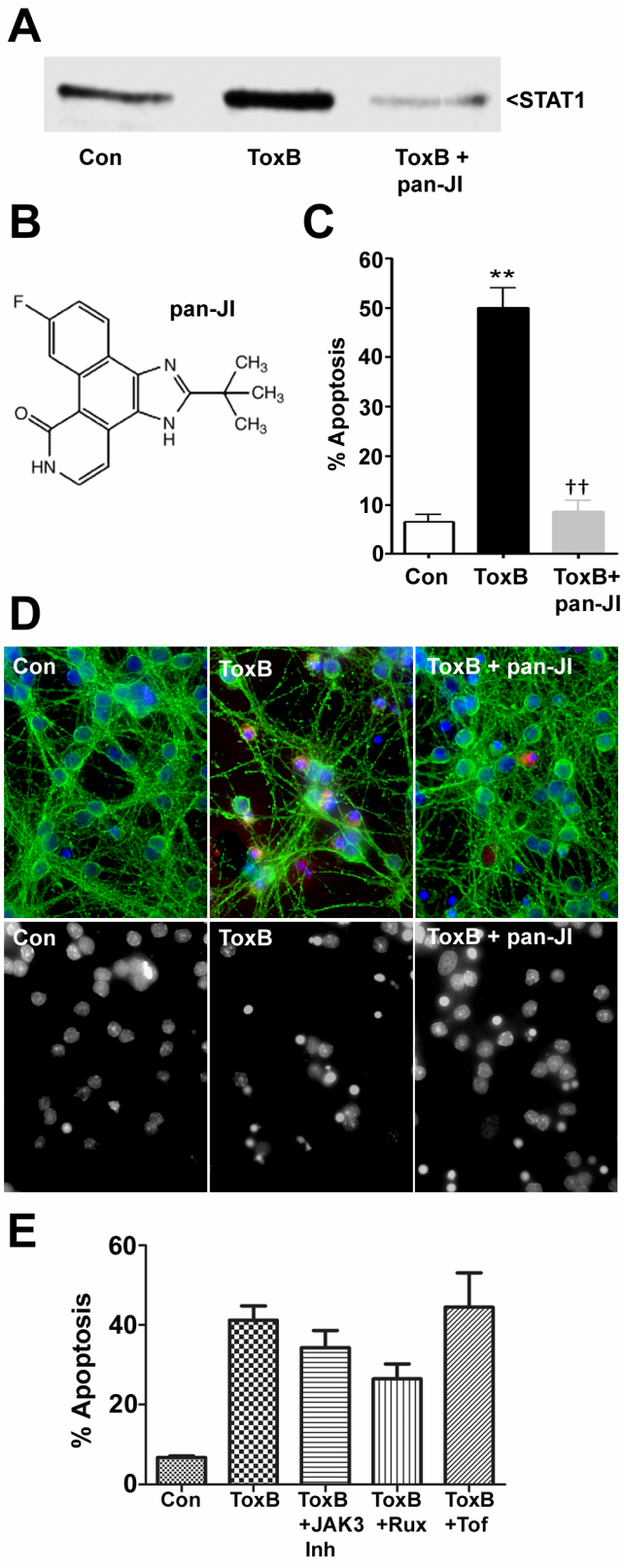
A
<STAT1
Con
ToxB
ToxB +
pan-JI
B
pan-JI
F
O
HN
N
H
N
CH3
CH3
CH3
C
% Apoptosis
60
50
40
30
20
10
0
**
††
Con
ToxB
ToxB+
pan-JI
D
Con
ToxB
ToxB + pan-JI
Con
ToxB
ToxB + pan-JI
E
% Apoptosis
60
40
20
0
Con
ToxB
ToxB
+JAK3
Inh
ToxB
+Rux
ToxB
+Tof

Figure 2

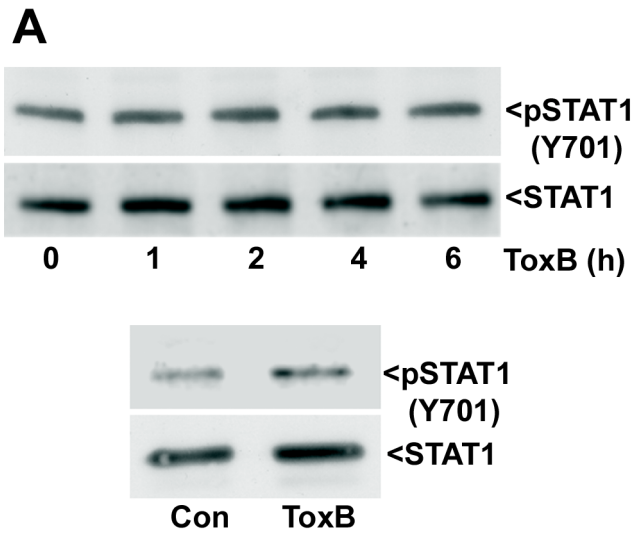
A
<pSTAT1
(Y701)
<STAT1
0
1
2
4
6
ToxB (h)
<pSTAT1
(Y701)
<STAT1
Con
ToxB
B
Con
ToxB

Figure 3

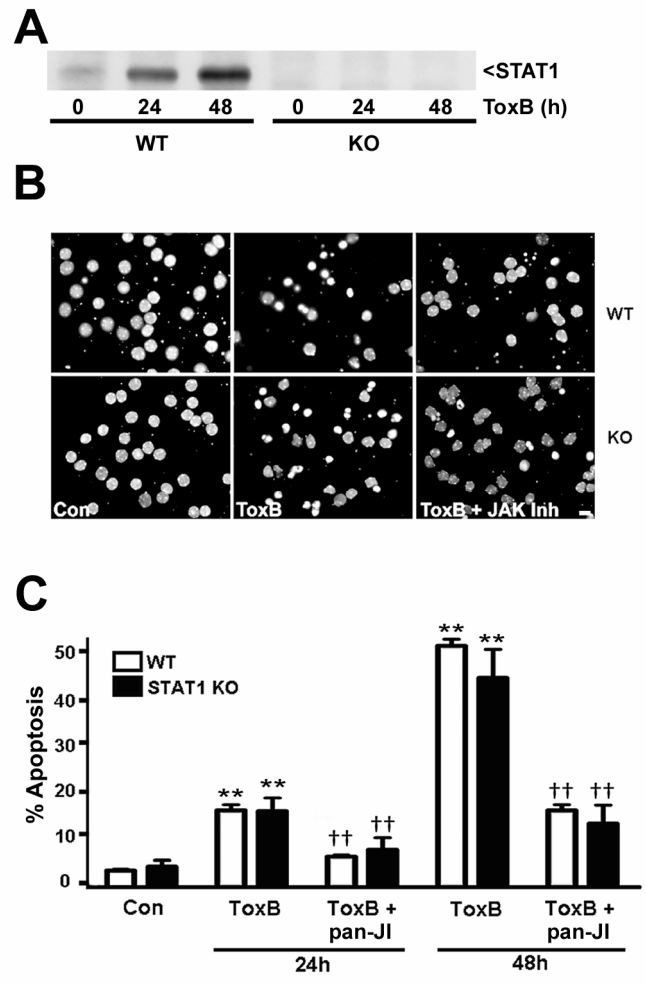
A
<STAT1
0
24
48
0
24
48
ToxB (h)
WT
KO
B
WT
KO
Con
ToxB
ToxB + JAK Inh
C
% Apoptosis
WT
STAT1 KO
Con
ToxB
ToxB + pan-JI
ToxB
ToxB + pan-JI
24h
48h

Figure 4

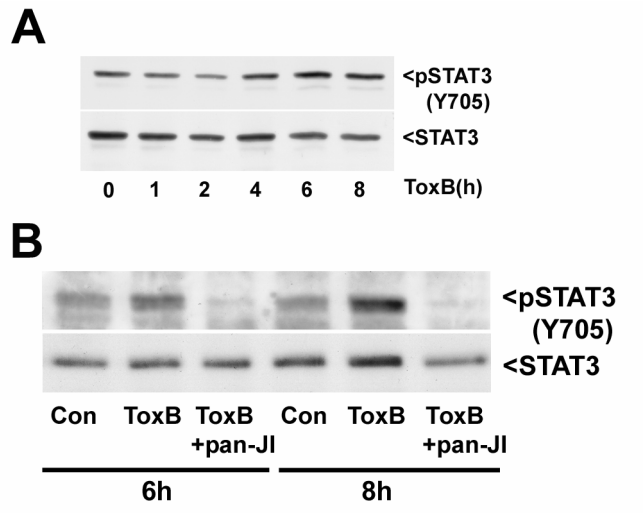
A
<pSTAT3
(Y705)
<STAT3
0 1 2 4 6 8 ToxB(h)
B
<pSTAT3
(Y705)
<STAT3
Con ToxB ToxB +pan-JI Con ToxB ToxB +pan-JI
6h
8h

Figure 5

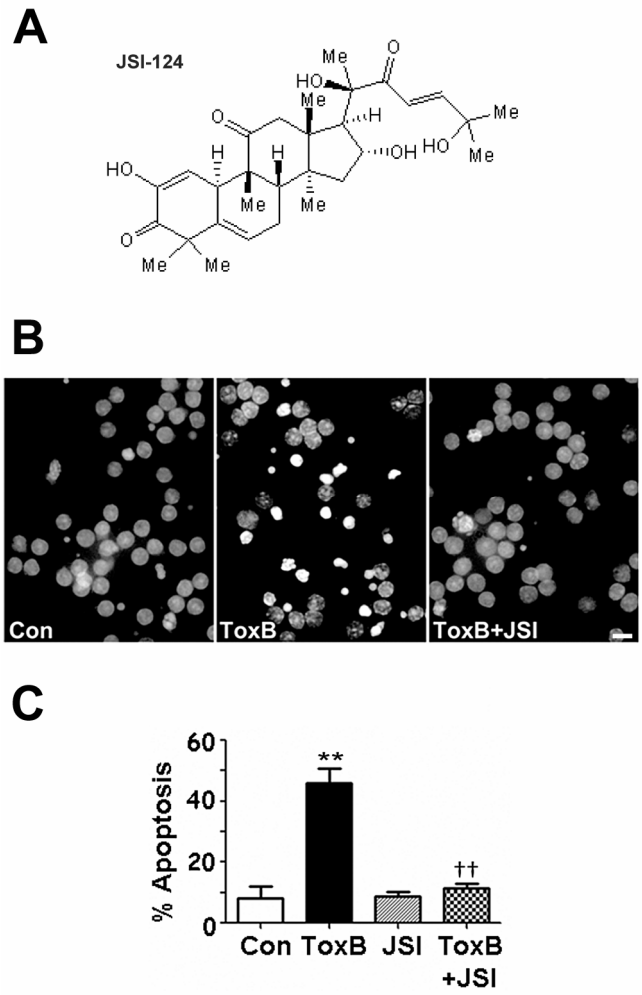
A
JSI-124
B
Con
ToxB
ToxB+JSI
C
% Apoptosis
60
40
20
0
**
††
Con
ToxB
JSI
ToxB
+JSI

Figure 6

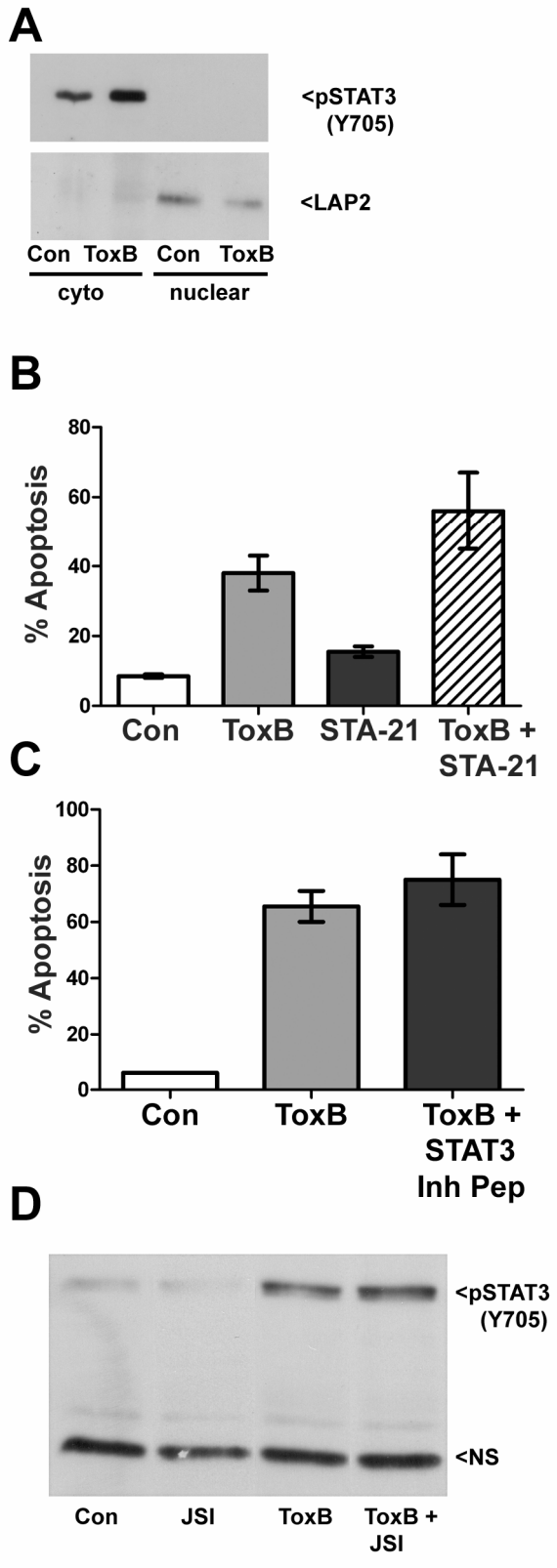
A
<pSTAT3
(Y705)
<LAP2
Con ToxB Con ToxB
cyto
nuclear
B
% Apoptosis
80
60
40
20
0
Con
ToxB
STA-21
ToxB +
STA-21
C
% Apoptosis
100
80
60
40
20
0
Con
ToxB
ToxB +
STAT3
Inh Pep
D
<pSTAT3
(Y705)
<NS
Con
JSI
ToxB
ToxB +
JSI

Figure 7

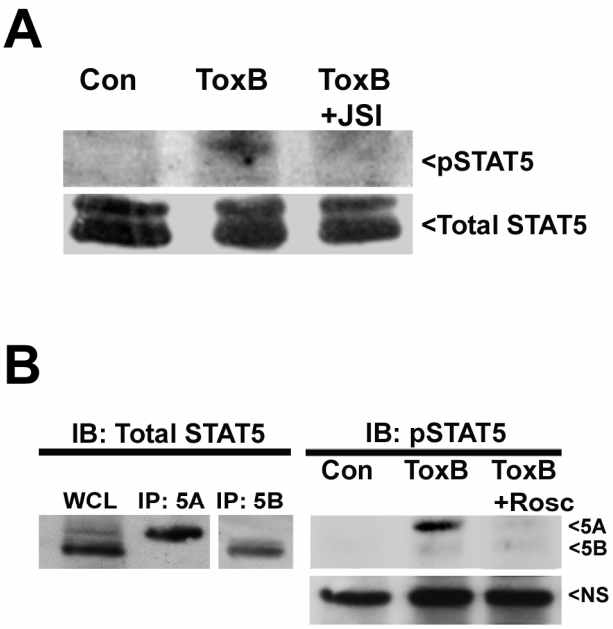
A
Con
ToxB
ToxB
+JSI
<pSTAT5
<Total STAT5
B
IB: Total STAT5
IB: pSTAT5
WCL
IP: 5A
IP: 5B
Con
ToxB
ToxB
+Rosc
<5A
<5B
<NS
C
Con
ToxB

Figure 8

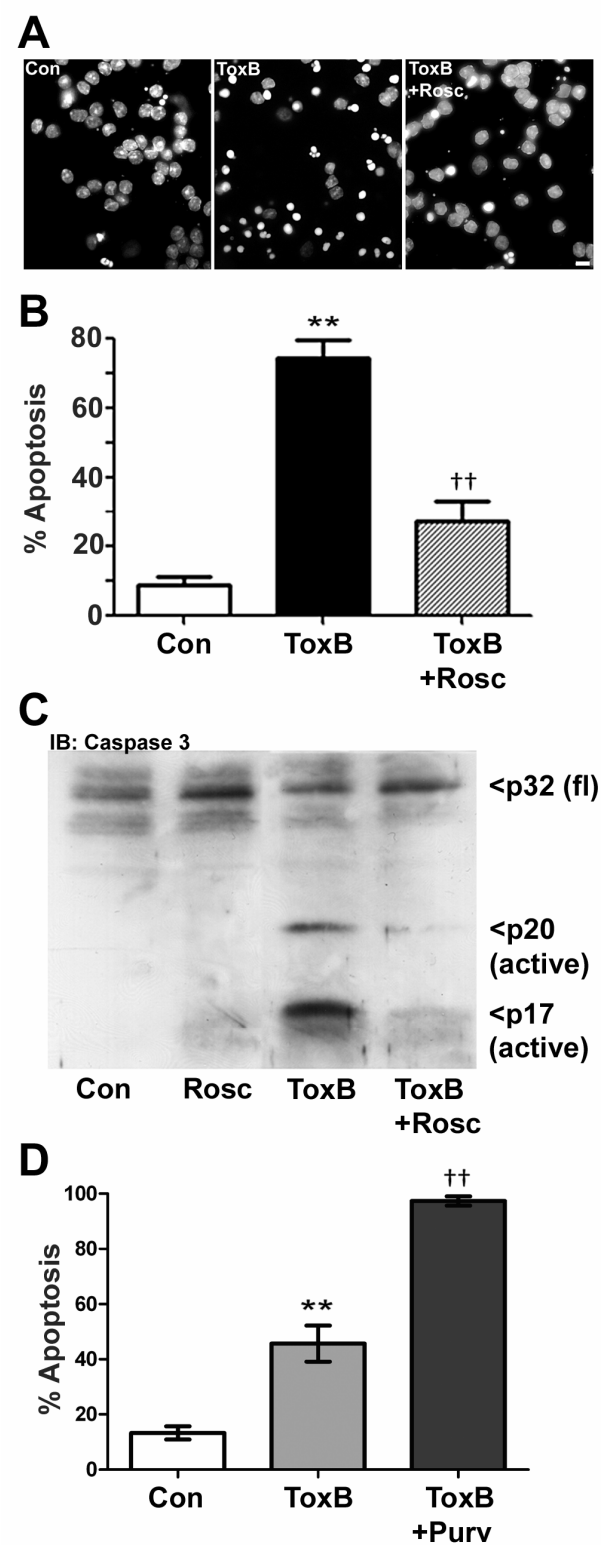

Figure 9

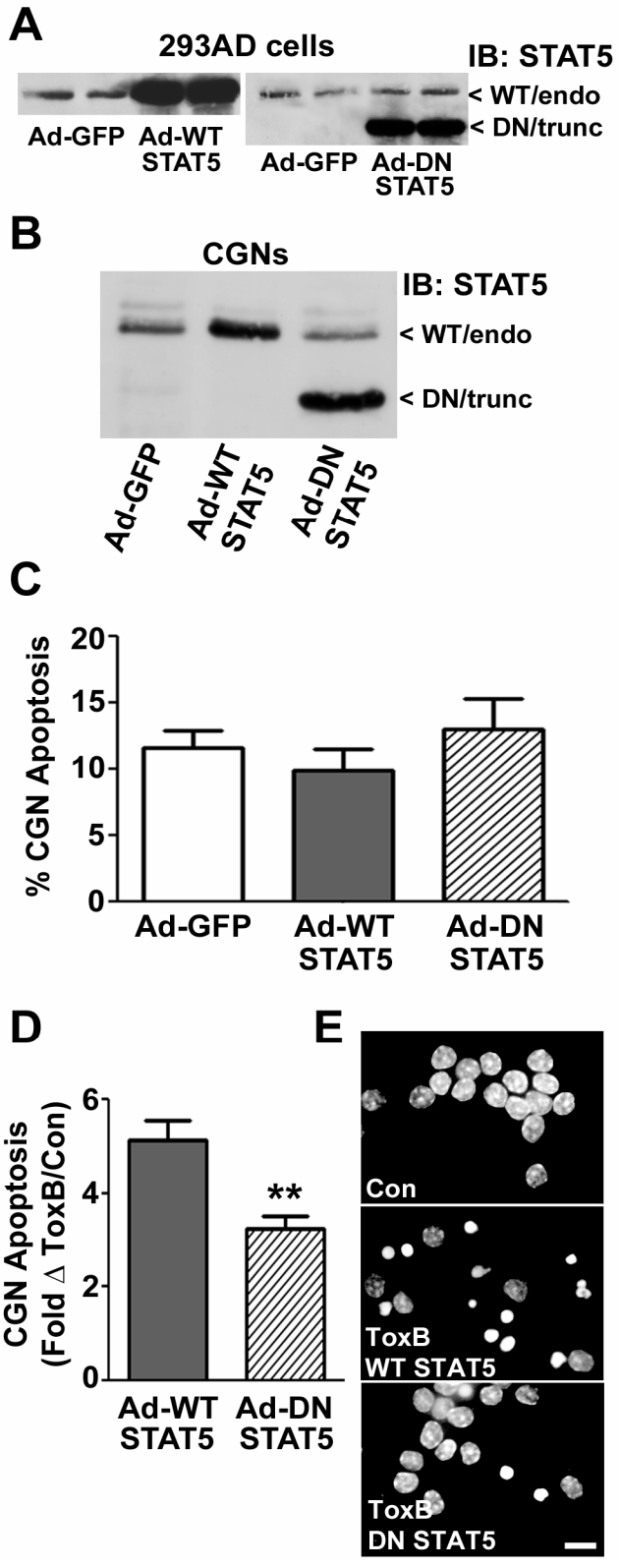
A
293AD cells
IB: STAT5
< WT/endo
< DN/trunc
Ad-GFP
Ad-WT STAT5
Ad-GFP
Ad-DN STAT5
B
CGNs
IB: STAT5
< WT/endo
< DN/trunc
Ad-GFP
Ad-WT STAT5
Ad-DN STAT5
C
% CGN Apoptosis
20
15
10
5
0
Ad-GFP
Ad-WT STAT5
Ad-DN STAT5
D
CGN Apoptosis (Fold Δ ToxB/Con)
6
4
2
0
**
Ad-WT STAT5
Ad-DN STAT5
E
Con
ToxB WT STAT5
ToxB DN STAT5

Figure 10

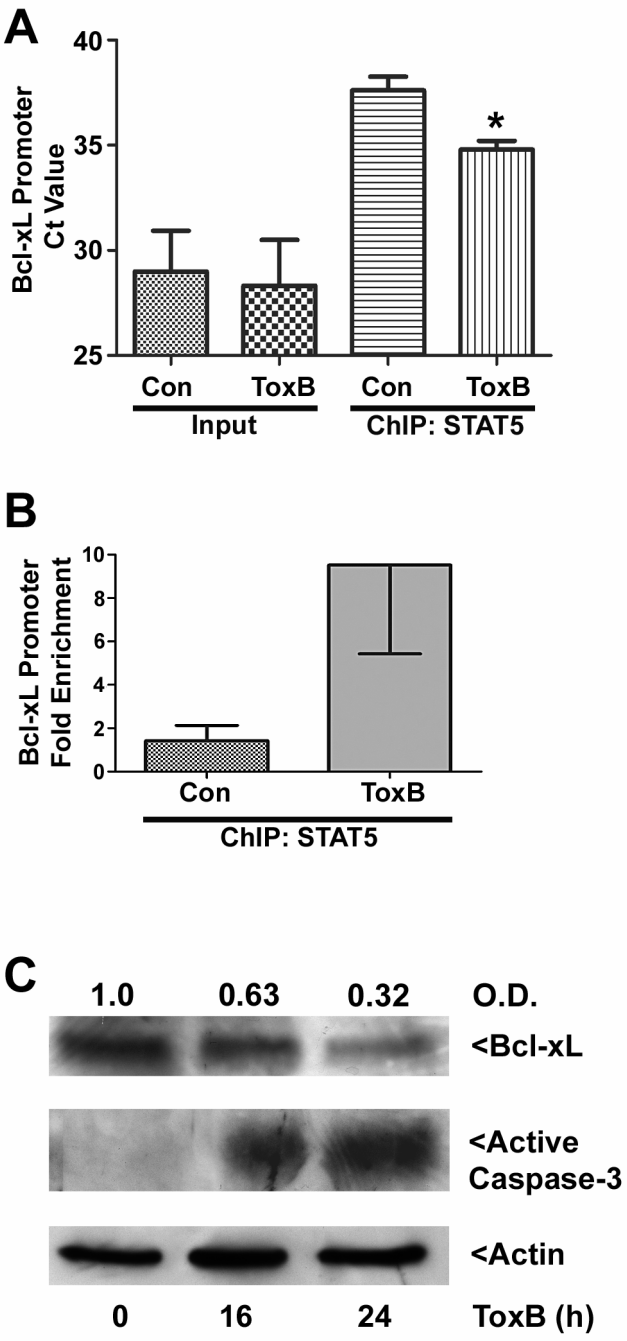
A
Bcl-xL Promoter
Ct Value
40
35
30
25
*
Con
ToxB
Con
ToxB
Input
ChIP: STAT5
B
Bcl-xL Promoter
Fold Enrichment
10
8
6
4
2
0
Con
ToxB
ChIP: STAT5
C
1.0
0.63
0.32
O.D.
<Bcl-xL
<Active
Caspase-3
<Actin
0
16
24
ToxB (h)